*Proceedings of the International Conference of Control, Dynamic Systems, and Robotics*
*Ottawa, Ontario, Canada, May 15-16 2014*
*Paper No. 115*

# Power Production for a Small-scale Experimental Hydrokite System

**Shriya S. Gosavi, Mario W. Gomes**
Rochester Institute of Technology, Department of Mechanical Engineering
76 Lomb Memorial Drive, Rochester, NY, USA 14623
ssg3175@rit.edu; mwgeme@rit.edu

***Abstract*** - Traditional hydropower systems have been used to generate power for centuries. Hydrokinetic systems, which do not require dams, have been recently developed and are gaining more interest due to their reduced ecological impacts. We show here a novel hydrokinetic system based on recently developed tethered airfoil wind power systems. This system consists of a hydrofoil attached to a rotating boom. Our initial experimental results for a small-scale system shows that, like the airborne kite systems, the power production is sensitive to hydrofoil angle. We have also determined that our small scale system can produce, if we neglect flipping losses, a maximum positive average cycle power of 0.6 W for a river flow rate of 0.5 m/s. Other tests were run where negative power was produced, *i.e.* power was absorbed with the hydrofoil flipping power being the likely source.

***Keywords:*** Hydropower, hydrokites, towtank, hydrofoil, energy.

## 1. Introduction

Most energy sources used today are dependent on fossil fuel reservoirs. Fossil fuels have a harmful effect on the environment and are requiring different and sometimes more complex technologies to mine them. Renewable energy sources like wind, solar and hydro power reduce our dependence on fossil fuels and have significantly less environmental impact. Conventional hydropower systems are a mature technology. These hydropower systems require expensive infrastructure and can only be cost-effectively built and operated at specific locations, most of which have already been exploited. In addition, there is active controversy about the negative ecological impact of dams on river ecology, such as interference with the fish migration cycle, increased sedimentation behind dams, and relocation of human populations (Bednarek, 2001). For these and other reasons, there has been a focused effort to develop new hydrokinetic systems to harness the power from moving water (rivers and tides), that don't require the use of dams. In this work, we introduce a novel hydrokinetic system which requires no dams and which we call a hydrokite.

The concept of this hydrokite system is based on the previously developed high-altitude tethered airfoil systems(Loyd, 1980; Lansdorp, 2005; Goela, 1986) which harness wind energy through the use of a tethered wing instead of a traditional tower and turbine. Jones *et al.* (1999) studied the power extraction efficiency of an oscillating wing generator undergoing a pitch and plunge motion. McKinney and DeLaurier (1981) performed experimental work on an oscillating wingmill having two degrees of freedom, a vertical plunging motion and a pitching motion. Unlike the system examined here, both of the systems studied by Jones and McKinney had short stroke lengths relative to the chord length of the wind or hydrofoil. McConnaughy (2012) examined, in simulation, an idealized version of our experimental system, depicted in Fig. 1. McConnaughy's steady-state simulation, provided an upper bound to the amount of power that can be produced from such a system. Parameters such as the boom angle and the hydrofoil flipping angle significantly influenced the predicted power production of this system. However, in the simulation several simplifying assumptions were made, the hydrofoil was assumed to flip instantaneously, the system was assumed to reach steady-state instantaneously, and the generator characteristics were assumed to be the same as for a generator operating at steady state. The experimental work presented here is not subject to any of those assumptions.

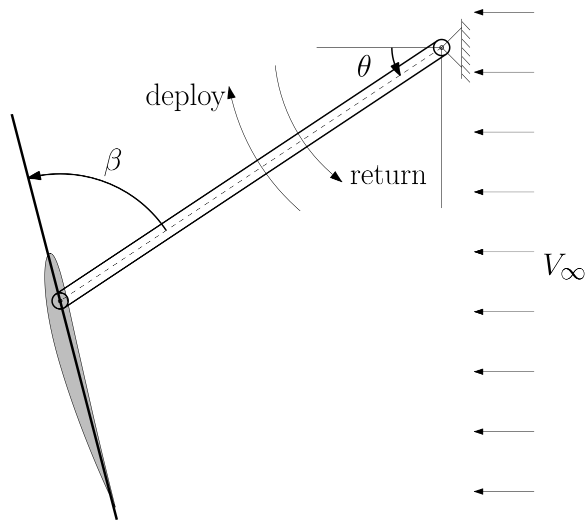


Fig. 1. Top view of hydrofoil and boom arrangement. The clockwise rotation to the side is the deploy stroke and the counter-clockwise rotation is the return stroke.

## 2. System Description

Our experimental set-up consists of a 5 m long tow-tank with a small-scale, instrumented hydrokite system. For all our tests using the tow-tank, instead of the test system remaining stationary and the fluid moving past it, we instead move the system though the stationary fluid. A top-view schematic of the experimental setup is shown in Fig. 2 and a photo of the small-scale rig is shown in Fig. 3. The tow tank has an attached cart which translates back and forth over the entire length of the tank. The cart is pulled by a 3/4 hp DC motor with a 12.5:1 gear reduction unit to decrease the rotational speed of the output shaft and increase its torque. A Dart Controls DC speed controller (MD 30E) was used to provide closed-loop PID control of the tow motor's angular velocity. This allowed us to specify a tow-speed and have that speed be maintained in the presence of loading disturbances, which is necessary given that the loading on the cart fluctuates during normal testing.

The small-scale testbed consists of a boom which is connected, via a pivot, to the base station located on the cart itself. A hydrofoil, which can pivot about its long axis and is controlled, is connected to the other end of the rigid boom. As the cart is moved at constant velocity, from one end of the tank to the other the hydrokite system reacts to the fluid forces being applied to the hydrofoil. Since the system is essentially a single degree of freedom system, the boom can only pivot on its supporting pin joint.

A simple feedback control system determines the angle of the hydrofoil during the motion. The angle of the hydrofoil is controlled, by the boom angle, to be in one of two specific positions and to change between those positions as quickly as our hardware will allow. This control system, along with the hydrodynamic forces applied to the hydrofoil, results in a stable periodic motion. This periodic motion, or cycle, consists of a deploy and return stroke for the boom. An electric generator is attached to the boom arm, via a gearbox, and resists the motion of the boom and generates electric power. For simplicity, and for future comparison to simulation results, we measure the mechanical power applied to the electric generator instead of the electric power produced from the generator.

The hydrokite system's performance is measured using two sensors. The angular position of the boom is measured via an encoder located on the generator at the pivot point of the boom arm. The torque applied to an electric generator located at the boom's pivot point is measured using a calibrated load cell. This load cell measures the tangential force required to keep the generator case from rotating. Knowing the value of the constraint force, which we measure, and the perpendicular distance from that force vector to the pivot point, the generator torque can be calculated. The instantaneous mechanical power produced by the system can then be calculated as the dot product of generator torque and boom arm angular velocity.

$$\vec{\tau} = \vec{r}_{p/o} \times \vec{F} \tag{1}$$

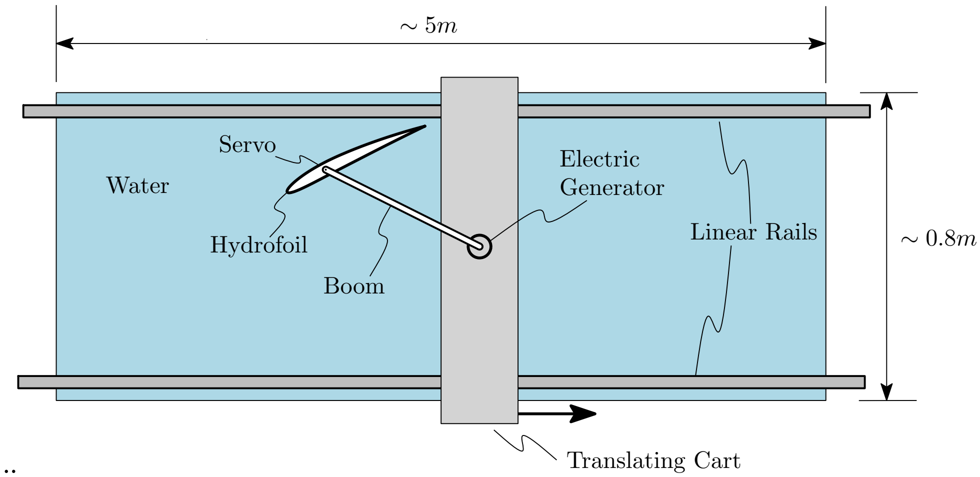


Fig. 2. Top view schematic of the tow-tank with small-scale hydrokite system used for the experiments.

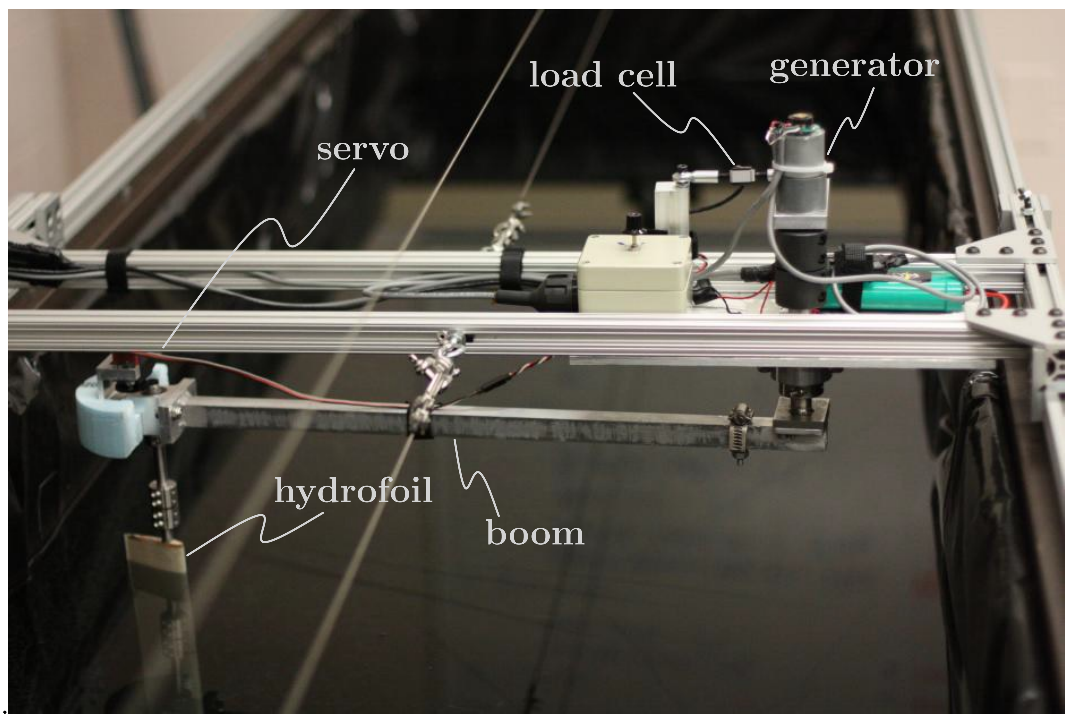


Fig. 3. The figure shows the boom and hydrofoil connections in the tank along with the load cell used to measure the forces, the generator, the encoder and the dump load. The system is present in the Energy and Motion Laboratory, Rochester Institute of Technology, Rochester.

$$P = \vec{\tau} \cdot \vec{\omega}_{boom} \tag{2}$$

The energy produced per cycle can then be calculated by integrating the instantaneous power over that cycle. The average cycle power can then be determined via Eqn. 3.

$$\bar{P} = \frac{\text{Energy per cycle}}{\text{cycle time}} = \frac{\int P dt}{T} \quad (3)$$

Data is collected using a NI data acquisition system (NI PCI-6229) with a LabVIEW interface. The boom angular position and generator torque are the only two variables which are sensed and measured. The hydrofoil angle is controlled via an RC digital servo (HobbyKing HK47011MG), which has its own closed-loop position feedback circuit to maintain the desired angular position. Due to the limited angular position range of this servo, we have used a gear reduction stage of 3:1 to allow the hydrofoil to rotate more than 180°. Data is collected every 1 ms. From this raw data, boom angular velocity is calculated which is used to determine the power generated.

Calculating velocity from experimentally obtained position data requires one of several techniques to reduce amplifying the noise that is naturally present in experimental data. We used the following procedure to differentiate the experimental data without unduly amplifying the signal's noise.

1. a window consisting of an odd number of data points is selected at the beginning of the dataset (21)
2. fit a polynomial function to those data points ($2^{nd}$ order polynomial)
3. analytically differentiate the polynomial function and evaluate it for the central data point in the window
4. shift the data window by one data point in the dataset and restart the procedure

### 2.1. Test Parameters

Several tests were carried out on the test bed. The parameters chosen for one of the tests, run #33, are listed in Table 1.

Table 1. List of parameters for the hydrokite system for Run #33

| Parameter | Value |
|---:|---|
| Hydrofoil (Airfoil shape) | NACA 0015 |
| Chord Length | 0.06 m |
| Hydrofoil Submerged Depth | 0.27 m |
| Flow Velocity | 0.5 m/s |
| Hydrofoil Deploy Angle ($\beta_d$) | 75° |
| Hydrofoil Return Angle ($\beta_r$) | $-55°$ |
| Flip Angle to Deploy ($\theta_d$) | 45° |
| Flip Angle to Return ($\theta_r$) | 15° |
| Mass of boom and servo | 0.850 kg |
| Mass of hydrofoil | 0.090 kg |
| Boom Length (from boom pivot axis to hydrofoil flip axis) | 0.51 m |
| Boom center of mass location (distance from boom pivot axis) | 0.434 m |
| Boom Moment of inertia of boom and servo about center of mass | $0.0089\ kg \cdot m^2$ |

Some of the parameters which we varied during our testing (along with the possible ranges for our testbed) were:

- Cart Velocity (0.1 m/s to 1.0 m/s)
- Hydrofoil shape (NACA0015 and NACA4412) [a symmetric and unsymmetric hydrofoil]
- Boom length (0.508 m, 0.381 m, 0.241 m )
- Chord length(0.071 m and 0.058 m )
- Hydrofoil Deploy/Return angles ($\beta$)
- Boom flipping angles for Deploy and Return ($\theta$)
- Hydrofoil submerged depth (0 m to 0.38 m)

## 3. Results and Discussion

Figs. 4 – 7 give the results, in detail, for a single representative test, run #33. Fig. 4 shows the two sensor signals for the entire test along with the desired hydrofoil angles (based on the simple flipping control algorithm described in section 2.) Fig. 4 also shows two marks which delineate the data which is later analyzed further in Figs. 5 and 7. Note that the dataset is clipped to remove the data transients from later analysis.

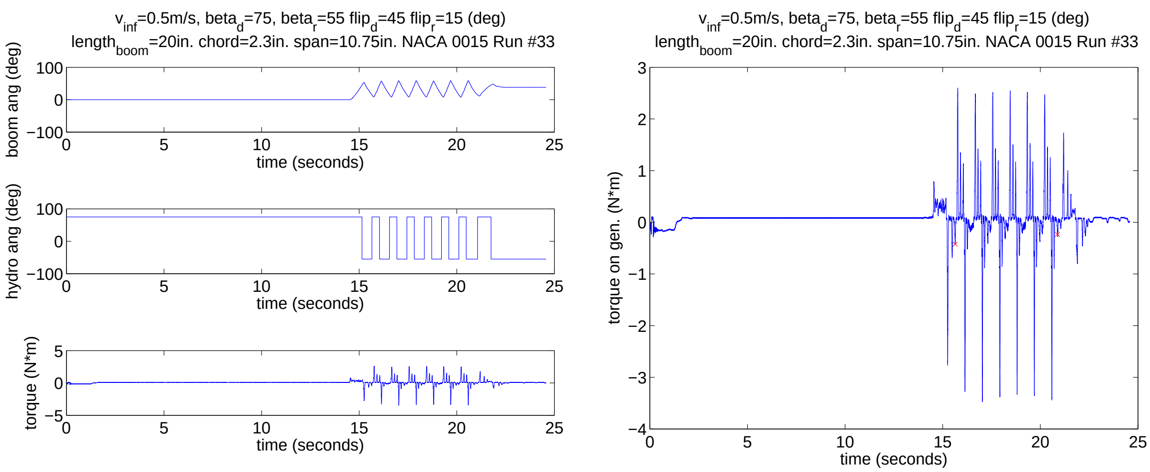


Fig. 4. Left plot shows the raw position and torque data collected from the sensors along with the desired hydrofoil angle. The two red marks delineate the clipped data which isolates the stable periodic motion of the system and ignores the data from the transient portions of the motion.

Fig. 5 shows the results of the numerical differentiation, described at the end of section 2, of the angular position data to obtain the boom angular velocity curve. Note that you can clearly see the slight fluctuations in the boom's angluar velocity both on the deploy and return stroke. Fig. 5 also shows a phase plane plot of the system's motion. Once the transients have been removed from the dataset, it is clear that the motion of the system is periodic and stable.

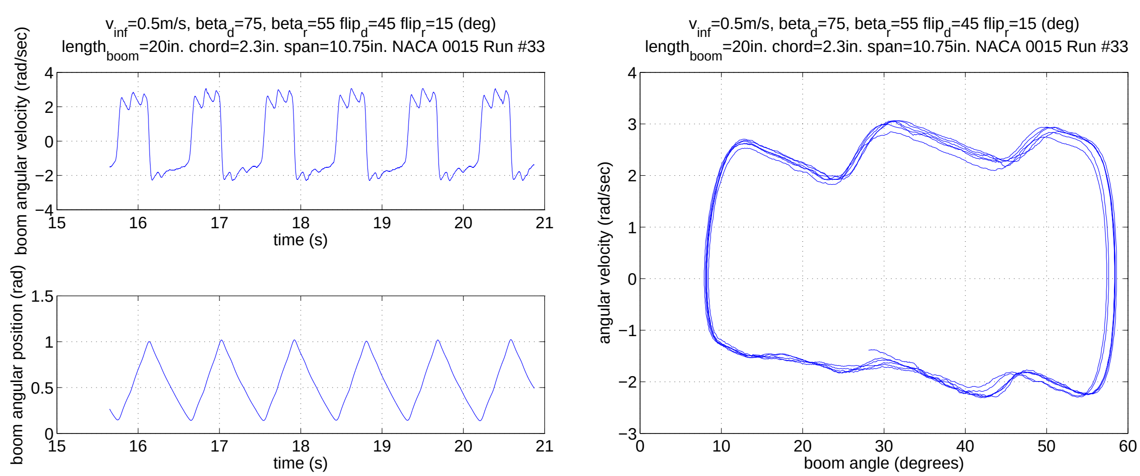


Fig. 5. Left plot shows the angular position of the boom along with the calculated time derivative of that signal. The right plot shows a phase plane plot of the periodic boom motion.

The relationship between the torque applied to the DC generator and the angular speed of the boom (as sensed by the encoder on the back of the DC generator) is shown in Fig. 6. Note that the relationship is significantly different from the idealized steady-state DC generator response which is also shown in Fig. 6. Note that the two small loops shown in Fig. 6 occur when the boom is moving across the width of the tank on the deploy and return strokes. These oscillations in boom velocity are due to, we conjecture, a combination of boom vibration and gearbox backlash. Note that the boom position is measured using an encoder which is mounted on the DC generator. In between the DC generator and the boom arm is a gearbox which is used primarily to increase the amount of torque applied to the boom arm. Thus any backlash between the input and output shafts of the gearbox will lead to errors in determining the true boom angular position. In addition, since the system's rotational motion changes direction each half cycle of operation, gearbox backlash can also affect the dynamics of the system itself.

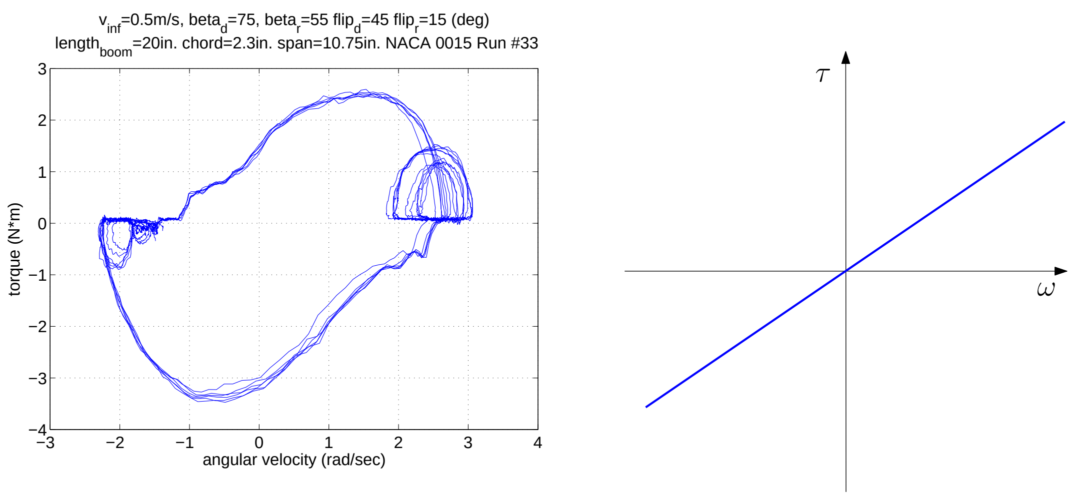


Fig. 6. Left plot shows that the dynamic response of the DC generator is significantly different from the linear steady-state response. The right plot shows a standard simplified steady-state generator response for a DC motor.

The instantaneous power produced by the system is calculated using Eqn. 2 and is shown in Fig. 7. One can clearly see that the instantaneous power fluctuates on both the deploy and return strokes. It is also clear that there are moments of negative power, where the system is doing work on the water instead of the water doing work on the system. Note that these negative power spikes occur during flipping of the hydrofoil. It is likely that the power used to flip the hydrofoil, which we have neglected, is contributing to these negative power spikes as measured at the generator.

Numerically integrating the instantaneous power for Test run #33 results in an average cycle power of approximately 0.6 W. However, we ran several other tests with different operating parameter values, some of which had a negative average cycle power. Table 2 shows the results of some of those tests. Note that all the tests shown in Table 2 use the following parameters:

- Hydrofoil shape (NACA0015 and NACA4412)
- Boom length is 0.508m
- Chord length is 0.071m
- Tow cart velocity of 0.5m/s

It is clear that for all the runs which produced negative average cycle power, that power must be coming from the power used to flip the hydrofoil at each end of the stroke. Thus, the power used for flipping the hydrofoil is not negligible. In addition, we note that the asymmetric hydrofoil appears to correlate exactly with negative power production. This somewhat odd result is, we believe, is due not to the shape of the hydrofoil, but instead due to placement of the pivot point on the hydrofoil itself. Our test hydrofoils were manufactured, due to strength and size requirements, with different pivot point locations. The symmetric NACA0015 hydrofoil pivot at the quarter-chord point, but the asymmetric hydrofoil pivots at the half-chord point. This change in pivot point significantly alters the

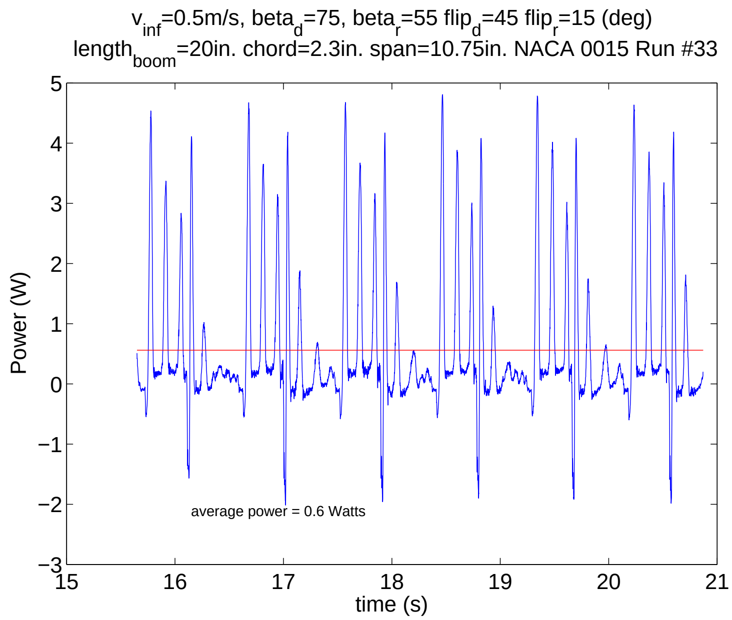


Fig. 7. Left plot shows that the dynamic response of the DC generator is significantly different from the linear steady-state response. The right plot show that the average cycle power for this run was 0.6 Watts.

Table 2. Combinations used for different runs for the hydrokite system producing positive and negative power

| $\lvert\beta_d\rvert$ | $\lvert\beta_r\rvert$ | $\theta_d$ | $\theta_r$ | Hydrofoil Profile | Average Cycle Power (W) |
|---|---|---|---|---|---|
| 15° | 25° | 45° | 20° | NACA 0015 | 0.4 |
| 25° | 25° | 50° | 20° | NACA 0015 | 1.9 |
| 15° | 25° | 45° | 15° | NACA 0015 | 0.8 |
| 25° | 25° | 50° | 15° | NACA 0015 | 0.7 |
| 65° | 55° | 50° | 20° | NACA 4412 | -0.3 |
| 65° | 55° | 50° | 15° | NACA 4412 | -0.5 |
| 75° | 55° | 45° | 15° | NACA 4412 | -0.5 |
| 75° | 55° | 45° | 20° | NACA 4412 | -1.1 |

flipping response of the two hydrofoils. Flipping a hydrofoil at the quarter-chord point can provide a force which has a large component that is perpendicular to the boom arm. This force can help accelerate the boom in it's motion back across the tank. On the other hand, this force component is significantly small for a hydrofoil which flips at the half-chord point. It appears that this change in pivot location is the dominant reason for the difference in power production between the symmetric and asymmetric hydrofoils, and not the change in shape between them.

### 3.1. Conclusions

The results show that an average cycle power of approximately 1.9 W can be produced by our small-scale hydrokite system in a flow velocity of 0.5m/s. However, this power production neglects the amount of energy required to flip the hydrofoil at the ends of the motion. Although the hydrofoil flipping power was not measured, we can infer from the negative average power production tests that this power is not negligible. We have also shown that this system is capable of stable periodic motions with a very simple control system. The power generated is sensitive to changes in operating parameters, with hydrofoil and boom flip angles being the largest influences on performance. Further testing is needed, with parameter optimization and additional sensing, before the system's maximum power production potential can be determined.

## Acknowledgments

We thank the following students for designing and building the tow-tank used in the experiments, designing and constructing the small-scale hydrokite testbed, and collecting the raw data: Hope Alm, Tim Buckner, Adam Dunn, Andrew Garland, Vulf Kirman, William Lentlie, Andres Santizo Matheu, Mark Negro, Shauna Traxler, and Michelle Wang. We also thank Ed Hanzlik for guiding the team and David Hathaway, Robert Kraynik, and Jan Maneti for machining help and construction advice. This work was funded in part by an EPA P3 grant #SU836021.

## References

Benarek A.T. (2001). "Undamming Rivers: A review of the ecological impacts of dam removal". Environmental Management, 27, 6, 803-814.

Goela J.S., Vijaykumar R., Zimmermann R.H. (1986). "Performance characteristics of a kite-powered pump". Journal of Energy Resources Technology, 108,2,188-193.

Jones K.D., Davids S., Platzer M.F. (1999). "Oscillating-wing power generation". Proceedings of the 3rd ASME/JSME Joint Fluids Engineering Conf, San Francisco, California.

Lansdorp B., Ockels W. (2005). "Comparison of concepts for high-altitude wind energy generation with ground based generator". Proceedings of the NRE 2005 Conference, Beijing. pp. 1-9.

Loyd M.L. (1980). "Crosswind kite power". Journal of Energy, pp.106-111.

McConnaghy K. (2012). "Analysis of translating hydrofoil power generation systems (Hydrokites)", Master's Thesis, Rochester Institute of Technology.

McKinney W., DeLaurier J. (1981). "The wingmill: An oscillating-wing windmill". Journal of Energy, pp. 109-115.